CHAPTER 2

An inverse algorithm for reconstructing an initial Tsunami waveform

Tatyana Voronina
Institute of Computational Mathematics and Mathematical Geophysics SB, RAS, Russia.

Abstract

This chapter proposes a new approach to reconstructing the initial tsunami waveform in a tsunami source area, which is based on the inversion of remote measurements of water-level data. The inverse problem in question is treated as an ill-posed problem of the hydrodynamic inversion with tsunami tide gauge records; hence, it imposes some restrictions on the use of mathematical techniques. Tsunami wave propagation is considered within the scope of the linear shallow-water theory. Numerical simulation is based on the finite difference algorithm and the method of splitting. The ill-posed inverse problem of reconstructing initial tsunami waveforms is regularized by means of a least square inversion using the truncated singular value decomposition approach. This method allows one to control instability of the numerical solution and to win through to obtain an acceptable result in spite of the ill-posedness of the problem. Such an approach provides a more accurate insight into potentialities intrinsic of the sea level network – used as a database for reconstructing a tsunami source. The sea level data inversion due to the methodology suggested could be used to obtain appropriate assumptions about the static deformation in the source area, as initial condition for the tsunami generation and for the widespread numerical modeling of real historical tsunamis, to verify algorithms and codes in the tsunami research. The approach proposed could be particularly effective as one of the supplementary tools for the early warning against frequent and destructive near-field tsunamis.

1 Introduction

People are surrounded by a variety of natural systems, the main part of them being guideless. Earthquakes and tsunamis just belong to such events. They bring disasters that cannot be completely prevented, but it is possible to mitigate them due

WIT Transactions on State of the Art in Science and Engineering, Vol 65, © 2013 WIT Press
www.witpress.com, ISSN 1755-8336 (on-line)
doi:10.2495/978-1-84564-770-4/002

to the timely prediction. What is a tsunami? It is now more important than ever to understand the nature and characteristics of tsunamis and their potential hazards to coastal communities.

The beginning of the new millennium was marked with a formidable challenge to humanity from the World Ocean. Thousands of miles from the scene could be seen in real time how the ruthless dark waters quickly and inexorably devour anything that until recently has been homes, gardens, fields – human life as is. Thus, on March 11, 2011, humanity saw terrible tsunami images of the coast of Japan. This day, a massive earthquake (9.3 Mw) has hit the northeast Japan, triggering a tsunami that has caused extensive damage. The giant waves deluged cities and rural areas, sweeping away cars, homes, buildings, a train, boats, leaving a path of death and devastation in its wake. More than 20,000 people were killed when the earthquake and tsunami struck. The tsunami in Japan recalled the 2004 disaster in the Indian Ocean. The Andaman tsunami that occurred on 26 December 2004 has caused severe damage to properties and the loss of 300,000 lives on the affected coastal regions – the deadliest tsunami in the world history. These mega-events served as a wake-up call to the coastal communities of many countries to stand up to the adverse impacts of future tsunamis. The first national tsunami warning system was organized in the late 1940s in the United States after the tsunami that occurred on Alaska Aleutian Islands, in 1946, and originally confined to the Pacific region; the system has been expanded to the Caribbean and the North Atlantic. The international Tsunami Warning Systems (TWS), involving 26 countries, was established after the Chilean tsunami in 1960, which generated a Pacific-wide tsunami causing extensive damage in various countries. Although not so frequent, destructive tsunamis have also generated in the Atlantic and the Indian Oceans, the Mediterranean Sea, and even within smaller bodies of water, like the Sea of Marmara, in Turkey. An early warning system for the Indian Ocean began operating in 2006. The absence of the tsunami warning system in the Indian Ocean in 2004 caused immense victims and highlighted the urgent need for robust international early warning systems. Today, a global international tsunami warning system acts under the auspices of the United Nations.

First of all, the mitigation of tsunami disasters demands modernization of the existing TWS which, in turn, requires scientific, engineering, and sociological research in order to assess probabilistic tsunami hazard coastal regions at risk and ultimately to produce appropriate inundation maps. All include an advanced technology of recordings of data of seismic, sea level, and pressure changes caused by tsunamis, on-line data processing with a greater accuracy.

It should be noted that tsunami warnings are extremely complicated, the statistics of issued warnings being far from satisfactory. For the last 55 years, up to 75% of warnings for regional tsunamis have turned out to be false, while each TWS has had at least a few cases of missing dangerous tsunamis, because seismic data often are translated to tsunami data not exactly. As a tsunami may be less than 1 m high on the surface of the open ocean, it is difficult to be noticed by sailors. The increasing reliability of the tsunami warnings can be achieved in part by numerical modeling, which allows estimating an expected propagation and run up, wave heights, inundation distances, current velocities, and arrival times of tsunami at the protected coastal communities.

The intensive development of numerical simulation of real tsunamis began in the late sixties of the twientieth century. Primarily, much attention was given to these problems in the Ring of Fire countries (USA, Japan, Canada, Australia, and Malaysia) and in Europe. Advanced computer technologies have given an impetus to the development of numerical modeling of tsunamis. The first studies in this area were carried out by Abe [1], Aida [2], Satake [5, 6] in Japan, by Mader [3], Bernard [4], Gonzalez *et al.* [7], Titov *et al.* [8, 9] in the United States, Tinti *et al.* [10] in Europe. They and other scientists have influenced on forming the TWS in all the countries.

In Russia, the study of the tsunami phenomenon started after the Kamchatka tsunami in 1952. Academician Soloviev [11] has pioneered some of the aspects of understanding and predicting tsunamis. Following his ideas several groups of scientists and specialists (in Moscow, Nizhny Novgorod, Leningrad, Novosibirsk, etc.) have studied at different times various aspects of this major problem. In the seventies of the previous century, numerous studies on the tsunami waves were carried out in scientific institutions of the Siberian Branch of the Russian Academy of Sciences to address the problems of numerical modeling of tsunami waves. Robust new computational algorithms and software were created by Gusiakov and Chubarov [12], Chubarov *et al.* [13, 14], Marchuk *et al.* [15], Hakimzyanov and Fedotova [16], etc. Commissioned by UNESCO the group headed by Shokin Y.Iv created the maps of the tsunami travel times (TTT) in the Pacific [17]. Their investigations correspond to the adopted concept of development of the National Tsunami Warning System of the Russian Federation. Their research has made possible evaluating tsunami risk through numerical simulation, in particular, estimating wave heights and run up for mitigation and warning. The specialized data-processing system WinITDB ITRIS (2007) and HTDB/WLD (2012), Historical Tsunami Database for the World Ocean (2012) (Web-version is available at http://tsun.sscc.ru/nh/tsunami.php) were pioneered by Gusiakov [18]. These information systems are developed by a tsunami research team for the purpose of the hydrodynamic modeling of tsunamis using computer models.

In case of a near field tsunami that are generated by sources located at short distances of less than 300 km and that are the most devastating, the disaster management has a little time for decision making. Mathematical modeling of tsunamis is to provide tsunami-resilient communities with reliable information of inundation heights and arrival times for the purpose to immediate protective measures. There are two important aspects of the assessment of tsunami risk in the coastal areas: the initial waves generated at the source area and provided further distractive strength of tsunami impact and the subsequent propagation. Generally accepted numerical tsunami models are based on the long-wave theory, valid for a small amplitude and nondispersive propagation within linear and nonlinear shallow water models and recorded either in the Cartesian or in the spherical coordinate system. There are many of actively used codes that are based on this theory.

One of the first among software was developed as a part of the IUGG / IOC Time Project with support from UNESCO program TUNAMI (Tohoku University's Numerical-Analysis Model for Investigation of Tsunami) and its modifications TUNAMI-N2 by Goto *et al.* [19]. This code was updated by many authors, one of

successful modifications was made by Kurkin *et al.* [20] in the Institute of Applied Physics in Russia.

The first version of the MOST model (method of splitting tsunami) was developed by Titov and Gonzalez [21]. Numerical simulation was based on the finite difference algorithm for the nonlinear equations and the method of splitting. Generation of the initial perturbation uses a script based on seismic models [21]. This MOST model takes into account the Earth's curvature to predict tsunami travel over a long open ocean distance. It also accurately predicts the water-surface elevation and wave heights. Generation of the initial perturbation uses a script based on seismic models Okada [22].

The software system NEREUS was created by Chubarov *et al*. [23] in the Institute of Computational Technologies SB RAS and based on a modified difference scheme of MacCormack for shallow water equations in a conservative form. This code could provide numerical modeling of propagation and calculating run up heights. Computational experiments are conducted for a representative set of model sources of different power and distance for the Far Eastern coast of Russia.

Usage of more complicated models allows retracing more details of the wave behavior for example, a weakly nonlinear model by Nwogu [24], a fully nonlinear potential flow theory that was used to reproduce details of breaking wavefronts Lynett and Liu [25] or Pelinovsky [26] the long-wave nonlinear-dispersion model of the tsunami.

The software code FUNWAVE was based on the nonlinear dispersive equations obtained [27], originally destined for the wave modeling in the coastal zone. However, further development of this approach makes possible to apply it to various cases of wave propagations and run up simulation. The integrated software code GEOWAVE [28] includes both the Tsunami Open and Progressive Initial Conditions System (TOPICS) and the fully nonlinear Boussinesq water wave model FUNWAVE. TOPICS [29] is used to obtain the initial condition for several parametric scenarios of tsunami generation: underwater slides, underwater slumps, debris flows, and pyroclastic flows. The tsunami source predicted by TOPICS is introduced as an initial condition into FUNWAVE.

An attempt to make a comparative estimate of the efficiency of the known computational models and programming systems of the hydrodynamic tsunami simulation based on these models was undertaken in Shokin *et al.* [30]. According to the results obtained, all the above-mentioned models are almost identical to the computational accuracy of the algorithms and to the hydrodynamic accuracy of mathematical models. This fact allows one to state that the effects of nonlinear dispersion terms are of minor importance of the overall wave behavior of concern, such as amplitudes and run up heights.

Apparently, the most effective approach to solving the problem of numerical tsunami simulation is to use various models at different stages of the tsunami wave existence.

This review of the currently known tsunami simulation software codes is far from being exhaustive and is intended to show the diversity of approaches. The list of commonly used hydrodynamic approaches and the modeling codes descriptions

for the problem of generation and propagation of the tsunami waves can be found, for example, in Levin and Nosov [31] and *Gusiakov et al.* [32].

Recently, the devastating tsunamis have acutely put forward the problem for their timely warning and, as consequence, the importance of the accurate tsunami simulation. It can be expected that the development of numerical modeling of tsunami waves will increase the reliability of tsunami forecasting. An important part of tsunami simulation is to gain some insight into a tsunami source. An earthquake occurred near the seabed may produce a co-seismic deformation that can cause a displacement in the sea floor that can in turn cause an initial sea surface deformation that result in a tsunami wave. This sea surface deformation will be called an initial tsunami waveform or simply a tsunami source. It is well known that only some time after an event, by analyzing various seismic, tidal, and other data, it becomes possible to estimate the tsunami source basic characteristics. Slow and often inaccurate estimation of the earthquake source parameters remains an obstacle to on-time tsunami predictions. Thus, a demand arose for a more effective method in the near-field, where a warning should be issued in 5–10 min. Numerical modeling of a tsunami source is an important tool of assessment and mitigation of the negative effects of tsunamis. The sea level data inversion could be used to obtain appropriate assumptions about the static deformation in the source area as initial condition for the tsunami simulation.

There are many approaches to creating the method based on the inversion of near-field water-level data.

Satake [5, 6] was the first to propose a tsunami waveform inversion method using Green's function technique to invert a co-seismic slip from observed tide gauges data. *A priori* information about the tsunami source played an essential role in his inversion method. It is quite a common practice to determine the slip distribution along the fault of tsunamigenic earthquakes on the basis of tsunami data, eventually using the joint inversion of tsunami and geodetic data. A similar approach was used by Johnson *et al.* [33, 34]. In the method proposed by Tinti *et al.* [10] and Piatanesi *et al.* [35], the inversion of tide-gauge records for the initial waveform determination was carried out by the least-squares inversion of a rectangular system of linear equations. One of the main advantages of this method is that it does not require *a priori* assumption of a fault plane solution: actually, this method is completely independent of any particular source model, but its serious limitation is using only the linear propagation models. An adjoint method for tsunami waveform inversion was proposed by Pires and Miranda [36] as an alternative to the technique based on Green's functions of the linear long wave model [5]. The tsunami's initial condition was searched by way of the optimization of the sets of unknown parameters of a linear or a nonlinear function defined as an initial state. This method has the advantage of being able to use the nonlinear shallow water equations, or other appropriate equation sets. A large number of papers is devoted to estimating the slip distribution of an earthquake in the tsunami center by the inversion of teleseismic body waves (Baba *et. al* [37]).

This chapter is concerned with a new approach to solving the problem of reconstructing a tsunami source. It is well known that the inverse problem at hand is

ill-posed, which imposes some restrictions on the use of mathematical techniques. To this end, we have developed a technique based on the least-squares inversion using the truncated singular value decompositio (SVD) approach. The inverse problem to infer the initial sea displacement is considered as a usual ill-posed problem of the hydrodynamic inversion of tsunami tide-gauge records. Mathematically, the forward problem, that is, the calculation of synthetic tide-gage records from the initial water elevation field, is based on a linear shallow-water system of differential equations in the rectangular coordinates. This system is approximated by the explicit–implicit finite difference scheme on a uniform rectangular grid; hence, a system of linear algebraic equations will be obtained. The ill-posed inverse problem is regularized by means of least-squares inversion using the truncated *SVD* approach. In this method, the inverse operator is replaced by its restriction to a subspace spanned by a finite number of the first right singular vectors [38]. The so-called *r*-solution [39] is produced by a numerical process. The quality of the solution is defined by relative errors of the tsunami source reconstruction.

On both practical and theoretical grounds it is of interest to answer the following questions: (1) What minimum number of the sea level records (marigrams) should be used to recover a tsunami source well enough? (2) How accurately a tsunami source can be reconstructed, based on recordings at a given tide gouge network? (3) Is it possible to improve the quality of reconstructing a tsunami source by distinguishing the most informative part of the initial observation system? For answering these questions within the framework of approach proposed, we have carried out a series of numerical experiments with synthetic data and a real bathymetry.

Based on the characteristics of a given tide gauges network, the proposed method allows one to control the numerical instability of the resultant solutions and hence to obtain an acceptable result in spite of the ill-posedness of the problem. The first few experiments have shown that this approach is effective in tsunami source reconstruction [38].

Thus, the results obtained strongly depend on the signal-to-noise ratio due to the ill-posedness of the problem. Since the tsunami wave is a low-frequency phenomenon as compared to the background noise, an appropriate filtering of the calculated signals was made. The numerical results have been found to be highly sensitive to the spatial distribution of the monitoring stations as related to the local bathymetric features. It was found, as in other methods, that the inversion skill of tsunami sources increases with the improvement of azimuthal and temporal coverage of assimilated tide gauges stations.

2 Statement of the problem

It is a normal practice to assume that a tsunami process onset is an abrupt displacement of huge volumes of water induced by the seafloor displacement when the seafloor is suddenly raised or lowered, or be caused by a violent horizontal displacement of water, as may occur in the case of a submarine landslide. Usually these sea floor movements may be triggered by seismic activities. An initial sea surface deformation is presumed to be equal to the co-seismic vertical

displacement of the sea floor. In view of the fact that most tsunamis that caused damage were generated by sources, located at short distances of less than 300 km, the curvature of the Earth is neglected in this research. This approach is widely applied to the numerical modeling of the tsunami generation.

Mathematically, the problem of reconstructing the original tsunami waveform in the source area is formulated as determination of spatial distribution of an oscillation source using remote measurements on a finite set of points, later called as "receivers." One of the most difficult and poorly understood aspects of the tsunami waves propagation is their interaction with the coastline. In this chapter, we have chosen the simplest of approximate models – with a condition of total reflection from the solid wall, consisting in nullifying the normal derivative of the function describing the free-surface elevation with respect to the external normal vector. Consider an xyz-coordinate system and direct the z-axis downwards. The plane $\{z = 0\}$corresponds to the undisturbed water surface. Consider the aquatic part Φ of a rectangular domain $\Pi = \{(x;y) : 0 \le x \le X; 0 \le y \le Y\}$on the plane $\{z = 0\}$with piecewise-linear boundaries on dry land Γ and straight-line sea boundaries. Let $\Omega = \{(x,y) : x_0 \le x \le x_M; y_0 \le y \le y_N)\}$ be a tsunami source subdomain of Φ. A tsunami is a series of waves traveling at high speeds, for long periods and with long wavelengths, generated by an abrupt displacement of large volumes of water in the ocean. The process of the tsunami wave initialization could be simulated within the scope of the shallow water theory, when water elevation $\eta(x,y,t)$ over the undisturbed state satisfies the following scalar wave equation:

$$\eta_{tt} = \operatorname{div}(gh(x,y)\operatorname{grad}\eta) + f_{tt}(x,y,t) \tag{1}$$

with initial condition:

$$\eta_{|t=0} = 0; \quad \eta_{t|t=0} = 0; \tag{2}$$

On the coastline, the total reflection condition is used, on the sea boundaries $\Gamma_1 : y = 0, \Gamma_2 : y = Y, \Gamma_3 : x = X$, absorbing boundary conditions are used (see [47]):

$$\begin{gathered} c_{\Gamma_1}\eta_{yt} + \eta_{tt} + \frac{c_{\Gamma_1}^2}{2}\eta_{xx}\,|_{y=0} = 0; \\ \frac{\partial\eta}{\partial n}|_{\Gamma} = 0, -c_{\Gamma_2}\eta_{yt} + \eta_{tt} + \frac{c_{\Gamma_2}^2}{2}\eta_{xx}\,|_{y=Y} = 0; \\ -c_{\Gamma_3}\eta_{xt} + \eta_{tt} + \frac{c_{\Gamma_3}^2}{2}\eta_{yy}\,|_{x=X} = 0; \end{gathered} \tag{3}$$

where c_{Γ_i} is the velocity on the appropriate boundary.

Water level oscillations $\eta_0(x,y,t)$, $0 \le t \le T$ are known on a line γ (a smooth curve without self-intersection)

$$\eta_0(x,y;t)|_{\gamma} = \eta_0(x(s),y(s);t); (x(s),y(s)) \in \gamma, 0 \le s \le S, \quad 0 \le t \le T. \tag{4}$$

In (1), $h(x,y)$ is the depth of the ocean, g is the acceleration of gravity, and function $f(x, y, t)$describes sea floor motion in the tsunami source area. The tsunami propagation velocity is defined as $c(x,y)=\sqrt{gh(x,y)}$. The above problem has a unique solution only if the source function allows factorization [40], that is, the time and spatial variables can be separated: $f(x,y,t)=H(t)\cdot\varphi(x,y)$, where $H(t)$ is the Heaviside step function. The function $\varphi(x,y)$ describes the initial sea surface deformation, which is a co-seismic vertical displacement of the sea floor. In addition, $\varphi(x,y)$ is supposed to belong to the class $C_c(\Omega)\cap\eta_2^1(\Omega)$.

3 Inverse method

Denote by A the operator of solution of the forward problem, which is defined by the following way: for each given $\varphi(x,y)$ solve the Cauchy problem (1)–(3) and restrict its solution to the line γ:

$$\mathcal{A}\varphi(x,y)=\xi(s,t). \tag{5}$$

We assume that function $h(x,y)$ is continuously differentiable (this assumption does not necessarily hold in the experiments). Then, as shown by Ladyzhenskaya [41, Ch. IV], a solution of the initial-boundary value problem (1)–(3) exists and belongs to an energy class of solutions. Consequently, the trace of this solution is defined for each $t\in(0,T)$ on the curve γ as an element of $W_2^{1/2}(\gamma(s),0\le s\le S)$ for sufficiently large S. In turn, as shown in [42] $W_2^{1/2}(\gamma(s),0\le s\le S)$ is compactly embedded in the space $L_2(\gamma(s))$. Thus, function $\xi(s,t)$ for each fixed t is an element of the space $L_2(0,L)$, and its norm continuously depends on t in this space. We can consider the operator A: $W_2^1(\Omega)\to L_2(\gamma\times(0,T))$ and the solution of equation (5) will be searched for in the least-squares formulation:

$$\phi_*(x,y)=\arg\min\left\|\mathcal{A}\phi(x,y)-\xi(s,t)\right\|_{L_2(\gamma\times(0,T))}$$

In [43], by means of a standard technique of embedding theorems, it was proved that the operator A is compact, but does not possess a bounded inverse. Therefore, any attempt to solve equation (5) numerically must be followed by some regularization procedure. In this chapter, a regularization is performed by means of the truncated SVD that leads to a notion of *r*-solution (see [39]).

4 *r*-solution

Shortly the notion of *r*-solution can be described as follows. It is known [44, Ch. IX] that any linear compact operator possesses a matrix representation, and the operator equation (5) can be rewritten as an infinite system of linear algebraic equations. It is also known that any compact operator is represented by a singular system $\{s_j,\vec{u}_j,\vec{v}_j\}$, $j=1,2,\cdots,\infty$, where $s_j\ge 0$, $s_1\ge s_2\ge\ldots\ge s_j\ge\ldots$ are singular values and $\vec{u}_j$ and $\vec{v}_j$ – left and right singular vectors. A very important property of the singular vectors is that they form bases in the data and model spaces, that

is, any functions $\varphi(x,y)\in W_2^1(\Omega)$ and $\xi(s,t)\in L_2(\gamma\times(0,T))$ can be presented as the Fourier series:

$$\varphi(x,y)=\sum_{j=1}^{\infty}\varphi_j\vec{v}_j;\quad \xi(s,t)=\sum_{i=1}^{\infty}\xi_i\vec{u}_i; \tag{6}$$

with $\varphi_j=(\varphi(x,y)\cdot\vec{v}_j(x,y))$ and $\xi_i=(\xi(s,t)\cdot\vec{u}_i(t))$. Taking into account these properties one can rewrite equation (5) in the "diagonal" form:

$$\mathcal{A}\left(\sum_{j=1}^{\infty}\varphi_j\vec{v}_j\right)\equiv\sum_{j=1}^{\infty}s_j\varphi_j\vec{u}_j=\sum_{i=1}^{\infty}(\xi(s,t)\cdot\vec{u}_i)u_i\equiv\sum_{i=1}^{\infty}\xi_i\vec{u}_i \tag{7}$$

and its solution is given by

$$\varphi(x,y)=\sum_{j=1}^{\infty}\frac{(\xi(s,t)\cdot\vec{u}_j)}{s_j}\vec{v}_j(x,y). \tag{8}$$

This solution is nothing but the normal general solution and the operator given by the right-hand side of (8) is the normal general pseudoinverse for the operator A (see [46]). As one can see from (8), the ill-posedness of the first kind operator equation with a compact operator is due to the fact that $s_j\to 0$ as $j\to 0$. Therefore, a small perturbation $\varepsilon(t)$ on the right-hand side $\xi(s,t)$ can lead to a rather large perturbation in the solution. It should be noted that the operator perturbation also leads to solution instability. The regularization procedure based on truncated SVD leads to the following notion of r-solution based on the relation:

$$\varphi^{[r]}(x,y)=\sum_{j=1}^{r}\frac{(\xi(s,t)\cdot\vec{u}_j)}{s_j}\vec{v}_j(x,y). \tag{9}$$

The r-solution is the projection of the exact solution on the subspace spanned by the r right singular vectors corresponding to the top singular values of the compact operator A. This truncated series is stable for any fixed parameter r with respect to perturbations of the right-hand side and operator itself (see [44]). It is reasonable that the larger r, the more informative the solution obtained. Finally, the value of r is determined by the singular spectrum and the data noise level.

5 Discretization of the problem

Any numerical method to solve (5) requires a finite-dimensional approximation. Since the operator A is compact, any finite-dimensional approximation, by a $K\times L$ matrix will converge to the operator, as $K, L\to\infty$ and also, $\varphi(x,y)^{KL}\to\varphi(x,y)$ (if it exists). Convergence of the r-solution of a finite-dimensional system of linear algebraic equations to the r-solution of an operator equation was carefully investigated in [44]. Let the domain Ω be a rectangle $[x_1,x_M]\times[y_1,y_N]$. In order to obtain a system of linear algebraic equations by means of a projective method, a trigonometric basis was chosen in the model space, that is, the unknown function $\varphi(x,y)$ has been represented as a series of spatial harmonics

$$\{\varphi_k(x,y) = \sin\frac{m\pi}{l_1}(x-x_c)\cdot\sin\frac{n\pi}{l_2}(y-y_c),$$

$$k = m\cdot n,\ n = 1,2,\cdots,N,\ m = 1,2,\cdots,M\}$$

with unknown coefficients $\{c_{mn}\}$:

$$\varphi(x,y) = \sum_{m=1}^{M}\sum_{n=1}^{N} c_{mn}\sin\frac{m\pi}{l_1}(x-x_c)\cdot\sin\frac{n\pi}{l_2}(y-y_c), \tag{10}$$

where

$$l_1 = (x_M - x_1);\quad l_2 = (y_N - y_1),\quad x_c = (x_1 + x_M)/2;\quad y_c = (y_1 + y_N)/2;$$

To sample the necessary data, consider an observation system of P receivers located at points (x_p, y_p), $p = 1,\ldots,P$. In this chapter, the free-surface oscillations $\eta_0(x_p, y_p, t)$ are assumed to be known for a finite number of times $\{t_j\}, j = 1,\ldots,N_t$ at each receiver. It is reasonable to choose a basis in the data space as a system of P vectors $\{\psi_l^{pj} = \delta_{lj}, l = p\cdot j, j = 1,\ldots,N_t, p = 1,\ldots,P\}$. From this, the dimensions of the solution and the data space are

$$\dim(\text{sol}) = K = M\times N;\qquad \dim(\text{data}) = L = P\times N_t;$$

Let us introduce a rectangular grid for the spatial variables and time. A uniform rectangular grid is defined in Π, with some grid points on the dry land. However, our difference scheme employs only grid points located in Φ. It seems more convenient to use the finite difference scheme not for equation (1) but for its equivalent first-order linear system in the unknown water elevation $\eta(x,y,t)$ and the velocity vector $(\zeta(x,y,t), \varsigma(x,y,t))$:

$$\begin{aligned} \zeta_t + g\eta_x &= 0 \\ \varsigma_t + g\eta_y &= 0 \\ \eta_t + (h\zeta)_x + (h\varsigma)_y &= 0 \end{aligned} \tag{11}$$

with initial conditions:

$$\eta\,|_t = 0 = \varphi(x,y),\qquad \zeta\,|_t = 0;\quad \varsigma\,|_t = 0. \tag{12}$$

We introduce the rectangular grid with the step Δx, Δy over the spatial variables and Δt over the time. Problems (11) and (12), boundary conditions (3) and condition (4) are approximated by an explicit–implicit finite four-point difference scheme on a uniform rectangular grid [15]. The scheme is of second-order accuracy with respect to the spatial variables and of first order with respect to time. The scheme is based on the so-called spaced pattern, which in combination with

central-difference approximation of spatial derivatives simplifies the numerical implementation of boundary conditions, as there is no need to define all the unknown functions on the boundary. As was mentioned earlier, the arrival of the wave on the coast is not considered in this chapter. Simulating the tsunami wave, we need approximation of two types of boundary conditions: (a) conditions on the coastal boundary are assumed to be the full reflection conditions; these are expressed by nullifying the derivative of $\eta(x,y,t)$ with respect to the external normal vector (3); (b) conditions on the so-called free boundaries due to an artificial restriction of a considered domain – the absorbing boundary conditions (*ABC*). In this chapter, we use the full absorbing conditions of second order of accuracy [47].

As a result the following system of linear algebraic equations in the unknown coefficients $\{c_k = c_{mn},\ k = m \cdot n,\ n = 1,\cdots,N,\ m = 1,\cdots,M\}$is obtained:

$$\mathbf{A}\tilde{\mathbf{c}} = \tilde{\mathbf{b}} \tag{13}$$

where

$$\tilde{\mathbf{b}} = (\eta_{11},\eta_{12},\ldots,\eta_{1N_t},\eta_{21},\ldots,\eta_{2N_t},\eta_{P1},\ldots,\eta_{PN_t})^T;$$

$$\eta_{pj} = \eta_0(x_p,y_p,t_j), p = 1,\ldots,P,\ j = 1,\ldots,N_t.$$

To obtain the matrix *A*, we solve numerically the direct problem (11), (12), and (3) where each of the basic function $\{\varphi_k\}$ is used instead of $\varphi(x,y)$. The matrix *A* is rectangular with SVD decomposition A = UΣVT, where dim(V) = K × K and dim(U) = L × L. The right singular vectors $\{\tilde{V}_k, k = 1,\ldots,K\}$ of the matrix *A* are columns of the matrix V, the left singular vectors $\{\tilde{U}_i, i = 1,\ldots,L\}$ are columns of the matrix U. Following (9) the vector $\tilde{c}$ is sought as the **r**-solution of system (13) in the form:

$$\tilde{\mathbf{c}}^{[r]} = \sum_{k=1}^{r} \frac{(\tilde{\mathbf{b}},\tilde{U}_k)}{s_k}\tilde{V}_k(x,y). \tag{14}$$

Then function $\varphi(x,y)$ is obtained as

$$\varphi(x,y)^{[r]} = \sum_{k=1}^{r} \frac{(\tilde{\mathbf{b}},\tilde{U}_k)}{s_k}\tilde{V}_k(x,y), \tag{15}$$

where $\tilde{V}_k(x,y) = \sum_{l=1}^{L} v_{kl}\varphi_l(x,y)$. The number *r* is taken as

$$r = \max\{k : \frac{s_k}{s_1} \geq \frac{1}{cond}\}, \tag{16}$$

where s_j are the singular values, and cond is the condition number of the matrix *A*, $s_k \geq 0$, $s_1 \geq s_2$, $\geq \ldots \geq s_k \geq \ldots$. It is clear that the properties of the matrix *A* and, consequently, the quality of the obtained solution are determined by the location and extent of the tsunamigenic area, configuration of the observation system, and

the temporal extent of the signal. Therefore, the singular spectrum obtained allows one to predict the potential result of reconstruction of the function $\varphi(x,y)$. For example, if the perturbation on the right-hand side $\vec{\mathbf{b}}(s,t)$ can be written in the form

$$\vec{\varepsilon}(t) = \sum_{j=1}^{L} \varepsilon_j(t)\vec{U}_j,$$

then the solution will take the form

$$\phi(x,y) = \sum_{k=1}^{K} \frac{b_k + \varepsilon_k}{s_k}\vec{V}_k.$$

In this case the perturbation in the solution has the form

$$\vec{\delta} = \sum_{k=1}^{K} \frac{\varepsilon_k}{s_k}\vec{V}_k.$$

It is clear that $s_j / \varepsilon_j \to 0$ as far as $s_j \to 0$ if $j \to \infty$ and it is necessary to limit the number of used basic vectors proceeding from the cond of a matrix was not very much. While carrying out numerical calculations only right-hand singular vectors with sequence numbers k agreeing with the relation $s_k / s_1 \geq d$ were used. So, the number r is defined from (16), where d = 1/cond was set in advance. It has been turned out that r, the number of right singular vectors used, is much less than the minimum of the matrix dimensions. The number r depends both on the singular spectrum of the matrix A and on the noise level of the signals observed.

6 Numerical experiments: description and discussion

A series of calculations was made by the proposed method aimed at recovering the unknown function $\varphi(x,y)$:

$$\varphi(x,y) = \beta(x,y) \cdot a(x), \tag{17}$$

where $a(x) = (x - x_0 + 3 * R_1) * (x - x_0 + R_1 / 6)$, and the function $\beta(x,y)$ describes a paraboloid:

$$\beta(x,y) = \begin{cases} 1 - \dfrac{(x-x_0)^2}{R_1^2} - \dfrac{(y-y_0)^2}{R_2^2} & , if \ \dfrac{(x-x_0)^2}{R_1^2} + \dfrac{(y-y_0)^2}{R_2^2} < 1 \\ 0 & , if \ \dfrac{(x-x_0)^2}{R_1^2} + \dfrac{(y-y_0)^2}{R_2^2} \geq 1. \end{cases}$$

Function $\varphi(x,y)$ (initial sea surface displacement) is in accord with a sea floor deformation of typical tsunamigenic earthquakes with reverse dip-slip or low-angle trust mechanisms.

The main goal of numerical experiments presented in the following was to analyze the influence of the observation system on the quality of the recovering of the initial tsunami waveform. First, the purpose was to obtain the acceptable result of the recovering with the minimum number of the used receivers. It is necessary to recognize that the results obtained strongly depend on the presence of disturbance since the problem is ill-posed. However, since a tsunami wave is usually a low-frequency wave packet (compared to the background noise), it is reasonable enough to apply frequency filtration of the observed signal (or synthetic marigrams in our case). An initial data smoothing was performed by using a method of grid function smoothing proposed by Tsetsoho and Belonosov (see [48, Ch. 3.3]). The idea of the original algorithm was to sew n-times differentiable local approximations of a grid function by the Partition of Unity Method. We made an appropriate two-dimensional-smoothing procedure (based on the aforementioned method) for the recovered tsunami waveform. In all calculations, the quality of the solution strongly depends on the number of receivers and their disposition and is evaluated as the relative errors (in the L_2-norm) for the source function.

In order to avoid influence of other factors, we supposed that the ocean depth is the function of one variable and it is equal to the distance from the coast. This assumption for the function $h(x,y)$ is in good agreement with the bottom topography of the Kuril–Kamchatka shelf zone. All sizes are measured in kilometers. The domain Ω was a rectangle of size $[100; 200] \times [50; 150]$; the center point of the tsunami source was $(x_c; y_c) = (150;100)$. Function $\varphi(x,y)$ was approximately sought for in form (10), where $M = 25$; $N = 11$, $R_1 = 25; R_2 = 50; \phi_m ax \simeq 0.73m$. The receivers were disposed in the interval [10;190] of the y-axis (the coastal line), the maximum number of them was $P = 19$. Let us say that this data set defines Model 1.

In Fig. 2 results of the inversion using 2, 3, and 5 marigrams are presented. Matrix A (as a real matrix) is of size 153×275 in the case of three receivers, and 255×275 in the case of five, with that in both cases cond $A > 100$. The marigrams were obtained as a result of solving the direct problem (11)–(12) with boundary conditions (3), perturbed by the background noise, that is, a high-frequency disturbance. In Model 1, all experiments presented here were made with the disturbance rate of 5% of maximum amplitude of the signal over all receivers.

In Fig. 3 relative errors (in L_2-norm) of the recovering of source function for Model 1 using two, three, and five receivers, as functions of receivers disposition, noise levels, and value of cond are presented.

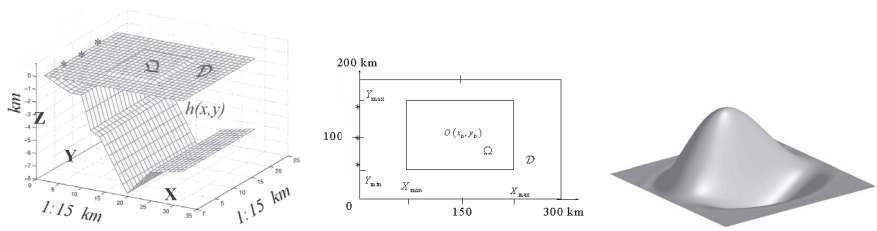

Figure 1: Model 1.

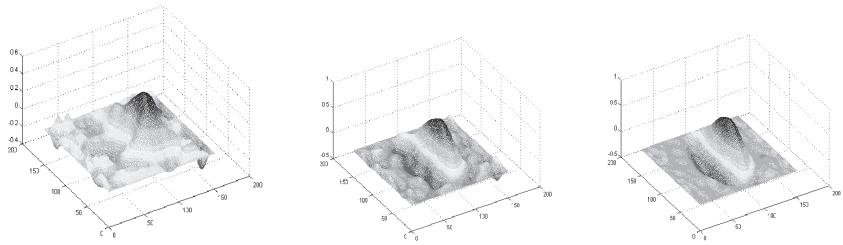

Figure 2: Recovered initial tsunami wave forms by the inversion using 2, 3, and 5 marigrams correspondingly for the numerical Model 1.

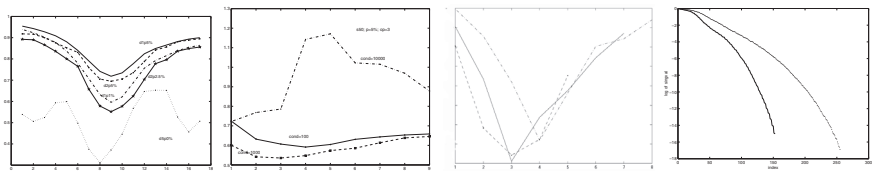

a) b) c) d)

Figure 3: the relative errors (in L_2-norm) of the recovering source functions for Model 1 with (a) two, (b) three, and (c) five receivers and singular values for the cases with (d) three and five receivers.

Namely, the curves in Fig. 3(a) show relative errors for the case when two receivers were used with different levels of the background noise and cond of the matrix A: 0%, cond = 10^5– red line; 5%, cond = 10^2 – blue line; 5%, cond = 10^3 – orange line; 2.5%, cond = 10^3 – green line; 1%, cond = 10^2 – brown line. Location of the first receiver was fixed at the initial point of the aperture (0,1), the second one was moved to the endpoint of the coastal segment with coordinates respectively (0, n). By the midpoint we mean the projection of the central point of the rectangle Ω (or the central point of the source, that is the same) onto the coastal line. Figure 2.3(b) corresponds to the case when there are three receivers positioned symmetrically with respect to the midpoint of the coast. In all experiments the horizontal axis points (n = 1,…9) were at the distance of $n \times 10$ km from the midpoint to the first supplemental pair of the receivers. The presence of a receiver in the midpoint has an essential influence on the results because the signal in this direction is mostly informative. It is typical for all calculations. Increasing of the cond implies increasing of the **r**-value and, hence, also informativeness of the solution. However, large oscillations appear in the numerical solution when cond is excessively large. The proposed approach allows one to control the accuracy by choosing the appropriate **r**-value. In Fig. 2.3(c) the relative errors are presented in the case of using five receivers in the following configuration: one plus two pairs. One of the receivers was also disposed at the midpoint while two pairs moved symmetrically to the endpoints of the coastal segment while the distance in every pair

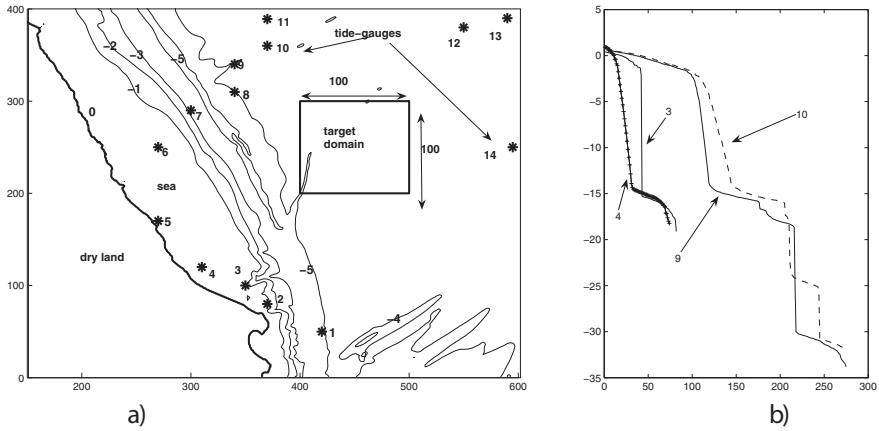

Figure 4: (a) Isolines of the Peru subduction zone with depth values, the target domain and the fourteen receivers marked by (*); (b) four graphs of singular values of the matrix A on a common log scale depending on their numbers. The numbers 3, 4, 9, 10 stand for the numbers of receivers used in certain appropriate variants of reconstruction.

is fixed this distance equals to 40 km (dashed line), 20 km (solid line), and 10 km (dashed-dot line). It is clear, that each of the represented lines has a point of the minimum value. In Fig. 3(d) natural logarithms of the singular values are presented for the cases of three and five receivers for Model 1.

The next data set Model 2 corresponds to the Peru coastal zone: as the function $h(x,y)$, the real Peru subduction zone was used. The domain Φ was the aquatic part of the rectangle $\Pi = \{0 \le x \le 600;\ 0 \le y \le 400\}$with piecewise-linear boundaries of dry land, the domain $\Omega = \{400 \le x \le 500;\ 200 \le y \le 300\}$ was a rectangle, see Fig. 4(a), the center point of a tsunami source was $(x_0;\ y_0) = (450;250)$, $R_1 = 40$; $R_2 = 50$ (all sizes are measured in kilometers). The maximum and minimum values of the function $\varphi(x,y)$ were $\varphi_{\max} = 1.959$ m; $\varphi_{\min} = -0.67$ m. $M = 25$; $N = 11$ were used in (10). $\Delta x = \Delta y = 1$ km were the space steps; hence, the domain Ω contained 100×100 mesh points. The time step was $\Delta t = 0.5sec$. Fourteen points in the domain Φ were chosen as receivers in the numerical experiments, thus $P = 14$. The time interval was taken large enough so that the tsunami wave reached all the chosen receivers, particularly, number of time steps was $N_t = 1684$. Hence, the following values of K and L: $K = 25 \cdot 11 = 275$, $L = 14 \cdot 1684$ were used. After specifying all the parameters the first step of numerical modeling was the calculation of synthetic marigrams in all receivers by solving the direct problem (11)–(12), (3) with $\varphi(x,y)$ from (17). Thus, the vector b in (13) was calculated. The second step was to calculate matrix A and then SVD decomposition by using a standard procedure. Thus, the singular spectrum that played a key role in estimating the quality of the reconstruction was obtained.

A series of calculations was carried out by the method proposed above to find a correspondence between certain characteristics of the observation system (such as,

e.g., the number and location of receivers) and results of the reconstruction process. Figure 4 shows (a) contour lines of the real bottom topography of the Peru subduction zone with depth values, the target domain and the 14 receivers enumerated clockwise and marked by (*); (b) typical graphs of common logarithms of singular values of matrix A depending on their numbers. The numbers 3, 4, 9, 10 stand for the numbers of receivers used in certain appropriate variants of reconstruction.

A sharp decrease in the singular values, when their number increases, is typical for all calculations, due to the ill-posedness of the problem. The parameter r in (14) is taken only from an interval, where the common logarithms of singular values are slightly sloping. It follows from Fig. 4(b) that only the number $r = 42$ was suitable for numerical modeling in appropriate variant with three receivers, that is, $P = 3$ and the number $r = 115$ can be used for the reconstruction with 10 receivers ($P = 10$). The performed numerical experiments show that using $r \leq 50$ will not produce an acceptable result. Comparison of the curves for three and four receivers show that the maximum allowable r (as well as properties of the matrix A) depends not only on the quantity of the receivers, but also on their azimuthal coverage. This dependence was investigated in detail in [48]. From the numerical experiments it is clear that a satisfactory parameter value is $r \geq 70$. Analysis of the singular spectrum of the matrix A can be extremely helpful for evaluating the real effectiveness of the tide gauges system for reconstructing the initial water displacement.

In the numerical calculations presented above the r-solution was obtained with cond ≥ 1000. The Table 1 shows how the configuration of the observation system affects the accuracy of tsunami source reconstruction. Here P is the quantity of receivers used in reconstruction; d is log(1/cond); err is the relative error (in the L_2 norm) of the reconstructed function; *f max*, *f min* are the extreme values of the function recovered. The last column shows the number of receivers used in the reconstruction in the order of increasing indices, according to Fig. 4.

Table 1: Influence of the observation system configuration, cond A and number r on the accuracy of the tsunami source reconstruction.

P	d	r	err	*f*max (m)	*f*min (m)	Number of receivers
	2	73	0.3767	1.559	–0.717	3, 4, 5, 6, 9, 10, 11
	2	55	0.4436	1.381	–0.768	2, 3, 4, 5, 6, 9, 10
	2	65	0.4588	1.449	–0.923	5, 6, 7, 8, 9, 10, 11
	3	93	0.3164	1.732	–0.6472	5, 6, 7, 8, 9, 10, 11
	4	99	0.2671	1.816	–0.7028	5, 6, 7, 8, 9, 10, 11
	2	42	0.552	1.276	–0.6745	1, 3, 5, 7 ,9 ,11, 13
	4	59	0.3173	1.706	–0.7371	1, 3, 5, 7, 9, 11, 13
	2	23	0.6278	1.106	–0.6959	3, 4, 5, 6, 7, 8, 9
	2	45	0.5752	1.431	–1.35	1, 2, 3, 5, 8, 9, 10
	2	66	0.6443	1.995	–1.920	1, 2, 3, 5, 9, 10, 11

In Fig. 5 the results of reconstructing of the function $\varphi(x, y)$ are presented for the inversion with nine marigrams for different groups of receivers and conditioning numbers of matrix A.

Synthetic marigrams were obtained by solving the direct problem (11)–(12), and (3) perturbed by a background noise. All experiments presented here were carried out with a noise rate of 3% of signal's maximal amplitude over all receivers. In Fig. 6 the initial and the recovered tsunami waveforms are presented.

The next step was solving the direct problem with the recovered and smoothed initial tsunami waveform to calculate marigrams at the same points as the synthetic ones. The results are presented in Fig. 3.

Each of the 14 pictures correspond to the receiver with the same number (see the location of receivers in Fig. 4). Some of the pictures presented here correspond to receivers used in reconstruction, but others correspond to the receivers which were not used called "rest." This means that the synthetic marigrams from the "rest" receivers were not used in formula (4), but the marigrams from the reconstructed tsunami source were calculated at these points. Denote (a) numerical reconstruction

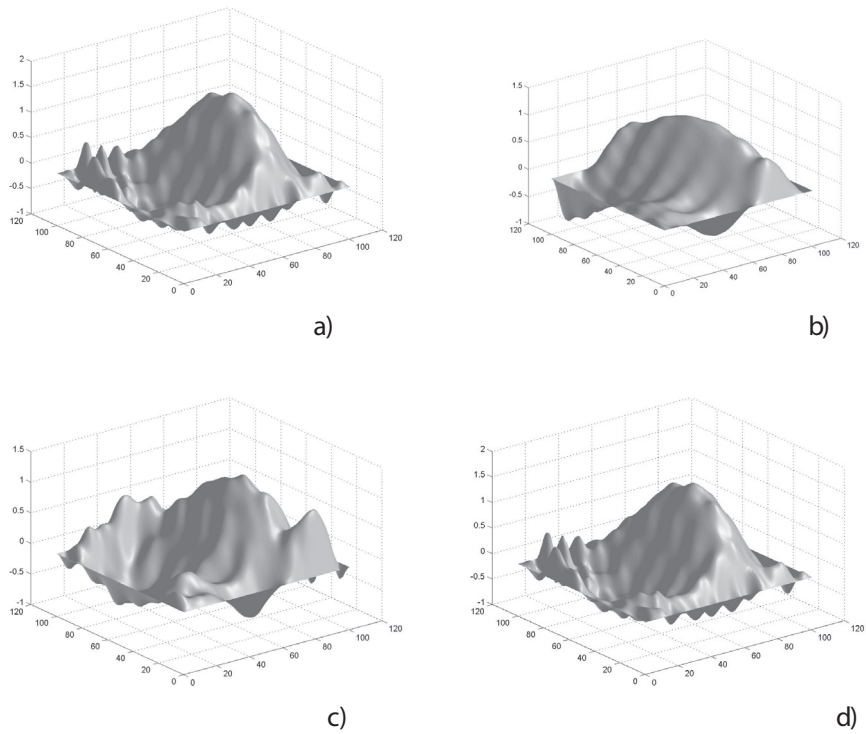

Figure 5: Reconstructed wave forms with nine receivers (a) receivers were used 3, 4, 5, 6, 7, 8, 9, 10, 11; cond = 1000; (b)receivers were used 2, 3, 4, 6, 7, 8, 12, 13, 14; cond = 1000; (c) receivers were used 3, 4, 5, 8, 9, 10, 11, 12, 13; cond = 1000.

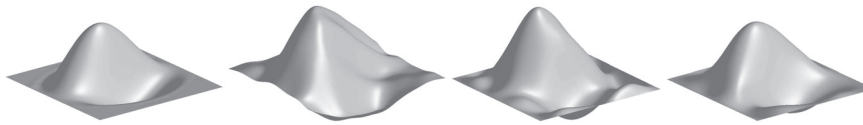

Figure 6: Wave forms (a) initial $\varphi_{\max} = 1.959\ m$; $\varphi_{\min} = -0.67\ m$; (b) three receivers, $\varphi_{\max} = 1.213(0.885)m$; $\varphi_{\min} = -0.738(-0.357)m$; $r = 41$; err. = 0.717; (c) five receivers, $\varphi_{\max} = 1.757(1.4716)m$; $\varphi_{\min} = -1.0073(-.5142)m$; $r = 57$; err. = 0.4729; (d) seven receivers, $\varphi_{\max} = 1.835(1.5138)m$; $\varphi_{\min} = -0.7016(-0.5484)m$; err. = 0.262; $r = 103$; log(1/cond) = 6. The values in parentheses are extreme values of the reconstructed waveforms after smoothing.

of a tsunami source by five marigrams from the receivers numerated as 3, 4, 6, 7, 10 as Model 2.1; (b) numerical reconstruction of a tsunami source by seven marigrams from the receivers numerated as 5, 6, 7, 8, 9, 10, 11 as Model 2.2. Every picture contains three graphs: the solid line denotes the synthetic marigram, the dashed line denotes the *marigram* for Model 2.1, and the dash-dotted line denotes the *marigram* for Model 2.2. One can see that Model 2.1 does not match sufficiently the marigrams. On the contrary, Model 2.2 gives a good agreement both for the receivers used in reconstruction and to the "rest" ones. This fact is very significant for the evaluation of the inverse algorithm. For predicting the water elevation in some area on the basis of data provided by some tide gauges the matching of marigrams is more important than the accuracy of reconstruction of a tsunami source. Our approach includes the following steps (1) calculation of the synthetic tide gauge records from a model tsunami source (2) reconstruction of the original tsunami waveform in the target domain by the inversion of marigrams; (3) calculation of the synthetic marigrams from the reconstructed source; (4) determining the most informative part of the observation system for a target area, for example, by comparing the marigrams obtained during previous steps in the same points; 5) setting up the observation system that contains only good-matching stations and reconstructing the tsunami source again, now using only these *nice* tide-gauge records. Obtained after step 5 improved tsunami source can be proposed for use in further tsunami modeling (tsunami wave propagation modeling, etc.).

7 Conclusion

In this chapter, a methodology was proposed for reconstructing initial tsunami waveforms in a tsunami source area based on remote measurements of water-level data. The approach is raised on SVD and *r*-solutions techniques, which are combined with a smoothing procedure to filter both the initial data and the reconstructed tsunami waveform. By analyzing the characteristics of a given tide gauges network, the above-proposed method allows one to control numerical instability of the solution and therefore to obtain an acceptable result in spite of the ill-posedness of the problem. The algorithm was verified by numerical simulating with real bathymetry of the Peru subduction zone and synthetic data. It has been

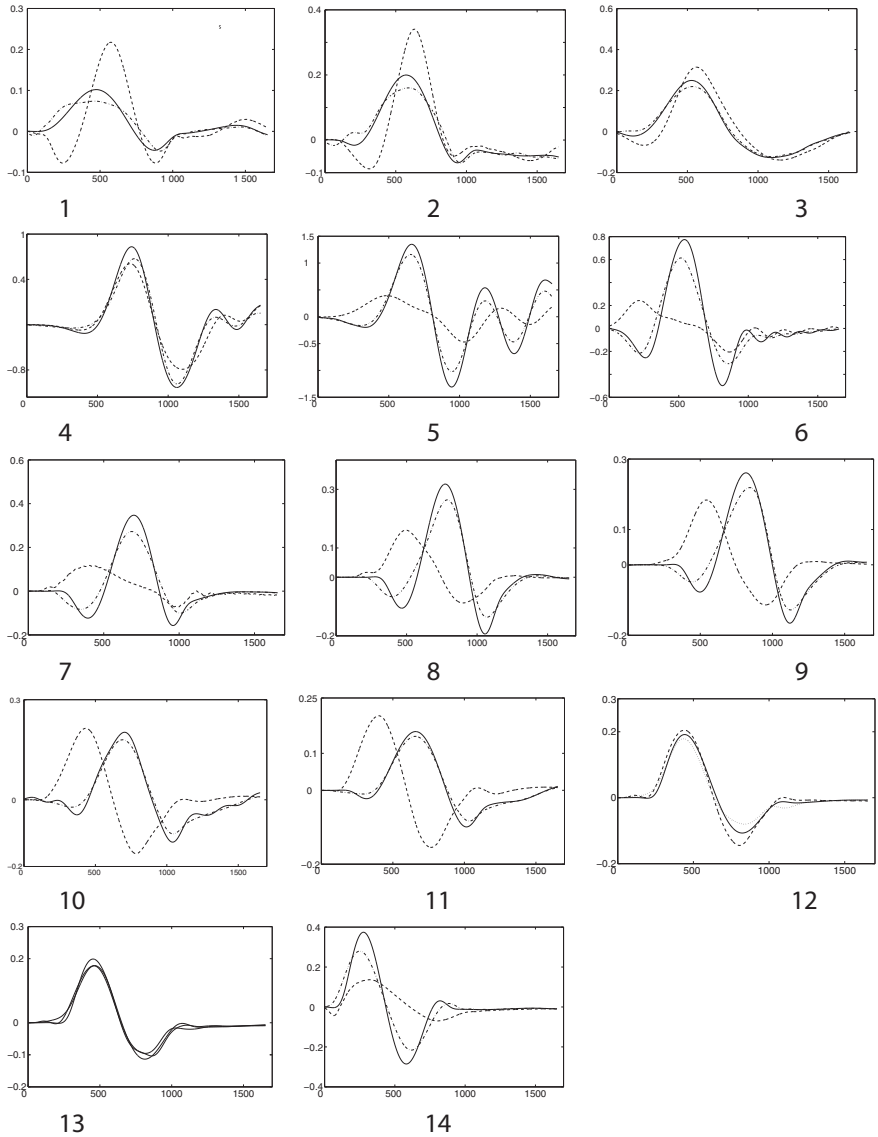

Figure 7: Marigrams in each of the fourteen receivers: the solid line denotes the synthetic marigram, the dashed line denotes the marigram for Model 1 (3, 4, 6, 7, 10 are the number of receivers); the dash-dotted denotes the marigram for Model 2 (5, 6, 7, 8, 9, 10, 11 are the number of receivers used). The horizontal axis is time, the vertical axis is tsunami wave height (m).

found out, that the accuracy of tsunami source reconstruction strongly depends on the signal-to-noise ratio, the azimuthal and temporal coverage of assimilated tide gauge stations relative to the target area and the bathymetric features along the wave path. The results thus obtained show that initial tsunami waveform reconstruction by the technique presented in this chapter has been successful.

Acknowledgements

This work was supported by the Russian Foundation for Basic Research under grant No 12-07-00406, by the Siberian Branch of the RAS (Project 117), by the Siberian Branch and the Far-Eastern Branch of the RAS Project 37), by the Ministry of Education and Science of Russian Federation (No. 16.740.11.0057).

References

[1] Abe, K., Tsunami propagation on a seismological fault model of the 1952 Kamchatka earthquake, *Bulletin of Nippon Dental University*, 8, pp. 3–11, 1979.
[2] Aida, I., Numerical computation of a tsunami based on a fault origin model of an earthquake, *Journal of the Seismological Society of Japan*, **27**, pp. 141–154, 1974.
[3] Mader, C.L., Numerical simulation of tsunamis. *Journal of Physical Oceanography*, **4(1)**, pp. 74–82, 1974.
[4] Bernard, E.N., A tsunami research plan for the United States. *Earthquake Engineering Research Institute*, **17**, pp. 13–26, 1983.
[5] Satake, K., Inversion of tsunami waveforms for the estimation of a fault heterogeneity: method and numerical experiments. *Journal of Physics of the Earth*, **35**, pp. 241–254, 1987.
[6] Satake, K., Inversion of tsunami waveforms for the estimation of hereogeneous fault motion of large submarine earthquakes: the 1968 Tokachi-oki and the 1983 Japan sea earthquake. *Journal of Geophysical Research*, **94**, pp. 5627–5636, 1989.
[7] Gonzalez, F.I., Bernard, S.N. & Milbern, H.B., et al., The Pacific Tsunami Observation Program (PacTOP). Proc. IUGG/IOC, Intern. Tsunami Simp., pp. 3–19, 1987.
[8] Titov, V.V. & Synolakis, C.E., Numerical modeling of tidal wave runup. *Journal of Waterway, Port, Coastal and Ocean Engineering*, **124(4)**, 157–171, 1998.
[9] Titov,V.V., Gonzalez, F.I., Bernard, S.N, Eble, M.C., Mofjeld, H.O., Newman, J.C.,& Venturato, A.J., Real-time tsunami forecasting: challenges and solutions. *Natural Hazards*, **35(1)**, Special Issue, US National Tsunami Hazard Mitigation Program, pp. 41–58, 2005.
[10] Tinti, S., Piatanesi, A. & Bortolucci, E., The finite-element wave propagator approach and the tsunami inversion problem, *Journal of Physics and Chemistry of the Earth*, **12**, pp. 27–32, 1996.

[11] Soloviev, S.L., The tsunami problem and its significance for the Kamchatka and the Kuril islands (in Russian), The Tsunami problem, Nauka, Moscow, pp.7–50, 1968.
[12] Gusyakov, V.K. & Chubarov, L.B., Numerical modeling of generation and propagation of tsunami in coastal zone, Izvestiya, Physics of the Solid Earth, **23(11)**, pp. 53–64, 1987.
[13] Chubarov, L.B. & Fedotova, Z.I., Numerical simulation of the long-wave runup on a coast. *Russian Journal of Numerical Analysis and Mathematical Modelling*, **18(2)**, pp. 135–158, 2003.
[14] Shokin, Yu.I., Chubarov, L.B., Fedotova, Z.I., Beizel, S.A. & Eletsky, S.V., Principles of numerical modeling applied to the tsunami problem. *Russian Journal of Earth Sciences*, American Geophysical Union, The World Publishing Service, 8, ES6004, doi: 10.2205/2006ES000216. ISSN: 1681-1208 (online), p. 23, 2006.
[15] Marchuk, An.G., Chubarov, L.B. & Shokin, Yu. I., *The Numerical Simulation of the Tsunami Wave*, Nauka Publishing House: Novosibirsk, pp. 369, 1983.
[16] Fedotova, Z.I. & Khakimzyanov, G.S., Nonlinear- dispersive shallow water equations on a rotating sphere. *Russian Journal of Numerical Analysis and Mathematical Modelling*. VNU Science Press BV, **25(1)**, pp. 15–26, 2010.
[17] Shokin, Y.I. & Chubarov, L.B. , Novikov, V.A. & Sudakov, A.N., Calculations of tsunami travel time charts in the Pacific Ocean - models, algorithms, techniques, results. *Science of Tsunami Hazards*, **5**, pp. 85–113, 1987.
[18] HTDB/WLD (2012), Historical Tsunami Database for the World Ocean (2012), Web-version is available at http://tsun.sscc.ru/nh/tsunami.php.
[19] Goto, C., Ogava, Y., & Imamura, F., Numerical method of tsunami simulation with the leap-frog scheme, (English translation and preparation by N. Shuto), in IUGG/IOC Time Project, IOC Manual and Guides, UNESCO, Paris 35, p. 126, 1997.
[20] Kurkin, A., Zaitsev, A., Yalciner, A. & Pelinovsky, E. Modified computer code "TSUNAMI" forevaluation of risks connected to tsunami. *Izvestia, Russian Academy of Engineering Sciences, Series: AppliedMathematics and Mechanics*, **9**, pp. 88–100, 2004.
[21] Titov, V.V. & Gonzalez, F.I., Implementation and Testing of The Method of Splitting Tsu-nami (MOST) Model, NOAA Technical Memorandum ERL PMEL-112, p. 11, 1997.
[22] Okada, Y., Surface deformation due to shear and tensile faults in a half-space. *Bulletin of the Seismological Society of America*, **75(4)**, pp. 1135–1154, 1985.
[23] Eletsky, S.V., Fedotova, Z.I. & Chubarov, L.B., Computer model of tsunami waves, *Proc. of Tenth Baikal All Russia Conf., Information and Mathematical Technologies in Science, Technology, and Education*, Part 1, ISEM, p. 138, 2005.
[24] Nwogu, O., Alternative form of Boussinesq equations for near shore wave propagation. *Journal of Waterway, Port, Coastal and Ocean Engineering*., **119(6)**, pp. 618–638, 1993.

[25] Lynett, P. & Liu P.L.F., A numerical study of submarine landslide generated waves and runup. *Proceedings of the Royal Society of London,* **458**, pp. 2885–2910, 2002.
[26] Pelinovsky, E.N., Tsunami Wave Hydrodynamics, Institute Applied Physics Press, Nizhny Novgorod, 1996 (in Russian).
[27] Wei, G. & Kirby, J.T., A time-dependent numerical code for extended Boussi- nesq equations. *Journal of Waterway, Port, Coastal, and Ocean Engineering*, **121**, pp. 251–261, 1995.
[28] Watts, P. & Grilli, S.T., Underwater landslide shape, motion, deformation, and tsunami generation , *Proc. of the 13th Offshore and Polar Engr. Conf.*, ISOPE03, Honolulu, Hawaii, 3, pp. 364–371, 2003.
[29] Watts, P., Grilli, S.T., Kirby, J.T., Fryer, G. J. & Tappin, G.R., Landslide tsunami case studies using a Boussinesq model and a fully nonlinear tsunami generation model. Natural Hazards and Earth Systems Sciences, **3**, pp. 391–402, 2003.
[30] Shokin, Yu.I., Babailov, V.V., Beisel, S.A., Chubarov, L.B., Eletsky, S.V., Fedo-tova, Z.I. & Gusiakov, V.K., Mathematical Modeling in Application to Regional Tsunami Warning Systems, Operations, Comp. Science and High Perf. Computing III, NNFM, Springer-Verlag: Berlin, Heidelberg, 101/2008, pp. 52–68, 2008.
[31] Levin, B.W. & Nosov, M.A., *Physics of Tsunamis*, Springer, p. 327, 2008.
[32] Gusiakov, VK, Yeletsky, S., Fedotova, Z.I. & Chubarov, L.B., Review and comparison of several software systems for simulation of the tsunami, *Proc. of the I(XIX) International Conference of Young Scientists*, devoted to the 60-anniversary of the Institute of Marine Geology and Geophysics FEB RAS, Study of natural catastrophes in Sakhalin and Kuril Islands (in Russia), Yuzhno-Sakhalinsk, pp. 214–221, 2007.
[33] Johnson, J.M.: Heterogeneous coupling along Alaska-Aleutian as inferred from tsunami, seismic and geodetic inversion. *Advances in Geophysics*, **39**, pp. 1–116, 1999.
[34] Johnson, J.M., Satake, K., Holdahl, S.R. & Sauber, J., The 1964 Prince William sound earthquake: joint inversion of tsunami and geodetic data, *Journal of Geophysical Research*, **101**, pp. 523–532, 1996.
[35] Piatanesi, A., Tinti, S. & Pagnoni, G., Tsunami waveform inversion by numerical finite-elements Green's Functions. *Natural Hazards and Earth System Science*, **1**, pp. 187–194, 2001.
[36] Pires, C. & Miranda, P.M.A., Tsunami waveform inversion by adjont methods. *Journal of Geophysical Research*,.**106**, pp. 19773–19796, 2001.
[37] Baba, T., Cummins, P.R, Hong Kie, T. & Hiroaki, T., *Validation and Joint Inversion of Teleseismic Waveforms for Earthquake Source Models Using Deep Ocean Bottom Pressure Records: A Case Study of the 2006 Kuril Megathrust Earthquake, Pure and Applied Geophysics*, Vol. 166. Springer, Birkhäuser-Verlag, pp. 55–76, 2009.
[38] Voronina, T. A. & Tcheverda, V.A., Reconstruction of tsunami initial form via level oscillation. *Bulletin of the Novosibirsk Computing Center Series Mathematical Modeling in Geophysics*, **4**, pp. 127–136, 1998.

[39] Cheverda, V.A. & Kostin, V. I., r-pseudoinverse for compact operators in Hilbert space: existence and stability. *Journal of Inverse and III-Posed Problems*, **3**, pp. 131–148, 1995.
[40] Kaistrenko, V. M., Inverse problem for reconstruction of tsunami source. *Tsunami Waves, Sakhalin Compl. Inst.Press*, **29**, pp. 82–92, 1972.
[41] Ladyzhenskaya, O.A., *Boundary-Value Problems of Mathematical Physics*. Springer: New York, pp. 407, 1985.
[42] Hormander, L., *The Analysis of Linear Partial Differential Operators*, Springer-Verlag: Berlin, 1983.
[43] Voronina, T, Reconstruction of initial Tsunami waveforms by a truncated SVD method. Journal of Inverse and III-posed Problems, **19(4–5)**, pp. 615–629, ISSN (Print) 0928-0219, 2011.
[44] Voronina, T.A., Determination of spatial distribution of oscillation sources by remote measurements on a finite set of points. *Siberian Journal of Numerical Mathematic (SibJNM),* Since 2008 the English version has been titling '*Numerical Analysis and Applications*' distributed by Springer, **3**, pp. 203–211, 2004.
[45] Kantorovich, L.V. & Akilov, G.P., *Functional Analysis*, Macmillan: New York, p. 650, 1964.
[46] Zuhair Nashed, M., Aspects of generalized inverses in analysis and regularization. *Generalized Inverses and Applications*. Academic Press: New York, pp. 193–244, 1976.
[47] Enquist, B., Majda, A., Absorbing boundary conditions for the numerical simulation of waves, Mathematics of Computation, **139**, pp. 629–654, 1977.
[48] Marchuk, G.I., *Methods of Numerical Mathematics*, Springer-Verlag: New York, Heidelberg, Berlin, p. 493, 1982.